



Active maintenance of endothelial cells prevents kidney fibrosis

Seung Hee Yang^{1,2,*}, Yong Chul Kim^{3,*}, Jung Nam An⁴, Jin Hyuk Kim¹, Juhoh Lee⁵, Hee-Yoon Lee⁶, Joo-Youn Cho⁷, Jin Ho Paik⁸, Yun Kyu Oh⁴, Chun Soo Lim⁴, Yon Su Kim^{1,9}, Jung Pyo Lee^{4,10}

¹Kidney Research Institute, Seoul National University Hospital, Seoul, Korea

²Seoul National University Biomedical Research Institute, Seoul, Korea

³Department of Internal Medicine, Seoul National University Hospital, Seoul, Korea

⁴Department of Internal Medicine, SMG-SNU Boramae Medical Center, Seoul, Korea

⁵Department of Chemistry, College of the Literature, Science and the Arts, University of Michigan, Ann Arbor, MI, USA

⁶Department of Chemistry, Korea Advanced Institute of Science and Technology, Daejeon, Korea

⁷Department of Clinical Pharmacology, Seoul National University College of Medicine, Seoul, Korea

⁸Department of Pathology, Seoul National University Bundang Hospital, Seongnam, Korea

⁹Department of Medical Science, Seoul National University College of Medicine, Seoul, Korea

¹⁰Department of Internal Medicine, Seoul National University College of Medicine, Seoul, Korea

Background: Soluble epoxide hydrolase (sEH) expressed by endothelial cells catalyzes the metabolism of epoxyeicosatrienoic acids (EETs), which are vasoactive agents.

Methods: We used a unilateral ureteral obstruction mouse model of kidney fibrosis to determine whether inhibition of sEH activity reduces fibrosis, the final common pathway for chronic kidney disease.

Results: sEH activity was inhibited by continuous release of the inhibitor 12-(3-adamantan-1-ylureido)-dodecanoic acid (AUDA) for 1 or 2 weeks. Treatment with AUDA significantly ameliorated tubulointerstitial fibrosis by reducing fibroblast mobilization and enhancing endothelial cell activity. In an *in vitro* model of endothelial-to-mesenchymal transition (EndMT) using human vascular endothelial cells (HUVECs), AUDA prevented the morphologic changes associated with EndMT and reduced expression of fibroblast-specific protein 1. Furthermore, HUVECs activated by AUDA prevented the epithelial-to-mesenchymal transition (EMT) of tubular epithelial cells in a co-culture system.

Conclusion: Our findings suggest that regulation of sEH is a potential target for therapies aimed at delaying the progression of kidney fibrosis by inhibiting EndMT and EMT.

Keywords: Epithelial-mesenchymal transition, Endothelial dysfunction, Endothelial-to-mesenchymal transition, Kidney fibrosis, Soluble epoxide hydrolase

Received May 31, 2017; Revised August 3, 2017;

Accepted August 15, 2017

Correspondence: Jung Pyo Lee

Department of Internal Medicine, SMG-SNU Boramae Medical Center, 20 Boramae-ro 5-gil, Dongjak-gu, Seoul 07061, Korea. E-mail: nephrolee@gmail.com

ORCID: <http://orcid.org/0000-0002-4714-1260>

*Seung Hee Yang and Yong Chul Kim contributed equally to this study.

Copyright © 2017 by The Korean Society of Nephrology

© This is an open-access article distributed under the terms of the Creative Commons Attribution Non-Commercial License (<http://creativecommons.org/licenses/by-nc-nd/4.0/>), which permits unrestricted non-commercial use, distribution, and reproduction in any medium, provided the original work is properly cited.

Introduction

Kidney fibrosis is the final common pathway of several types of kidney disease. Several mechanisms are involved in the onset and progression of fibrosis, including differentiation of infiltrating hematopoietic stem cells, proliferation of resident interstitial fibroblasts, and epithelial-to-mesenchymal transition (EMT) [1,2]. In addition, endothelial-to-mesenchymal transition (EndMT), a

process in which endothelial cells acquire mesenchymal characteristics, has recently been recognized as a crucial mechanism of fibrosis [3,4].

Endothelial cells are capable of releasing numerous vasoactive substances. Accordingly, endothelial cellular damage and impaired angiogenesis contribute to the progression of kidney failure. Epoxyeicosatrienoic acids (EETs), which are metabolites of arachidonic acid, are considered to be endothelium-derived hyperpolarizing factors (EDHFs) [5]. In this capacity, kidney EETs are involved in the regulation of kidney blood flow and long-term control of arterial blood pressure [6]. Soluble epoxide hydrolase (sEH) catalyzes the degradation of EETs to their corresponding diols and thus plays a central role in the regulation of EET levels. We recently demonstrated that treatment with sEH inhibitors can reduce acute kidney injury and evaluated the effects of genetic variants of sEH, encoded by the *EPHX2* gene, on the progression of immunoglobulin A nephropathy [7,8]. In the present study, we used a sEH inhibitor to investigate the roles of endothelial cells in the progression of kidney fibrosis.

Methods

Experimental animals and chemicals

Male C57BL/6 mice (20–22 g, 7–8 weeks old) were purchased from Orient Company (Seoul, Korea). All mice were raised in a specific pathogen-free animal facility. All experiments were performed under the approval of the Institutional Animal Care and Use Committee of the Clinical Research Institute at Seoul National University Hospital in accordance with the National Research Council ‘Guidelines for the Care and Use of Laboratory Animals’ [9]. The adamantyl alkyl urea-based sEH inhibitor 12-(3-adamantan-1-ylureido)-dodecanoic acid (AUDA) was synthesized by one of the co-authors of this study as described previously [8,10]. AUDA was dissolved in (2-hydroxypropyl)- β -cyclodextrin (cyclodextrin; Sigma Chemical Co., St Louis, MO, USA) at 45 mg/mL.

Induction of kidney fibrosis

Unilateral ureteral obstruction (UUO) was used as a model of kidney fibrosis in C57BL/6 mice. Mice were anesthetized with ketamine (100 mg/kg body weight) and

pentobarbital sodium (50 mg/kg body weight, Nembutal; Abbott, Wiesbaden, Germany). After left-flank incisions, UUO was achieved by ligating the left ureter with 4-0 silk at two points and cutting between the ligatures. Mice were placed on a heating pad (40°C) throughout the procedure. Sham-operated mice underwent identical surgical procedures except for ligation of the ureter. The sEH inhibitor AUDA (8 mg/kg/day) was continuously administered via an Alzet[®] implantable subcutaneous mini-osmotic pump (DURECT Co., Cupertino, CA, USA) for 1 or 2 weeks. The dose of AUDA was selected based on data from published studies [11,12]. Mice were sacrificed at the indicated times after induction of UUO. Blood pressure was measured before sacrifice using a non-invasive system (Kent Scientific Co., Chicago, IL, USA). Five-to-six mice were used for each group, and three independent experiments were performed for each procedure.

Tissue histology

Mice were sacrificed 1 or 2 weeks after UUO, and kidneys were harvested after exsanguination. Tissue samples were fixed with 10% buffered formalin, followed by paraffin embedding. Paraffin sections (4 μ m) were then stained with periodic acid-Schiff reagent and Masson’s trichrome staining. Tubulointerstitial lesion indexes were assessed semi-quantitatively from Masson’s trichrome-stained paraffin sections at 100 \times magnification [13]. A total of 10 fields per kidney were examined by a kidney histologist blinded to the treatment groups, and lesions were graded from 0 to 3 (0, no changes; 1, changes affecting < 25% of the section; 2, changes affecting 25–50% of the section; and 3, changes affecting 50–100% of the section), according to the area with tubulointerstitial lesions (tubular atrophy, casts, interstitial inflammation, and fibrosis). The score index for each mouse was expressed as a mean value of all scores obtained.

Cell culture

Human vascular endothelial cells (HUVECs; Cambrex, Walkersville, MD, USA) were cultured for four to six passages in EGM-2 MV medium (Clonetics Co., San Diego, CA, USA) supplemented with 10% fetal bovine serum, 1 mg/mL hydrocortisone, 12 mg/mL bovine brain extract, 50 mg/mL gentamycin, 50 ng/mL amphotericin B, and 10

ng/mL epidermal growth factor. After 3 days of culture, cells were detached from dishes by the addition of 3 mM ethylenediaminetetraacetic acid solution and a minimal amount of trypsin. Cells (2×10^5 /well) were then placed in 8-well chamber slides with serum-free medium for 24 hours and washed twice with phosphate-buffered saline (PBS). Next, recombinant transforming growth factor (rTGF)- β 2 (R&D Systems, Minneapolis, MN, USA) was added at a final concentration of 10 ng/mL, except where otherwise indicated. Cells were then incubated with or without AUDA (3 or 6 μ M) for 48 hours. Primary human tubular epithelial cells (hTECs) were isolated from unaffected specimens of surgically resected kidneys from patients diagnosed with kidney cell carcinoma [14]. hTECs were cultured for four to six passages in EGM-2 MV medium under the same conditions used for HUVECs.

Confocal microscopy

Confocal microscopy was performed using an LSM 510 meta laser confocal microscope (Carl Zeiss, Jena, Germany). For immunofluorescence studies, kidneys were snap-frozen in optimal cutting temperature embedding medium (Miles Inc., Elkhart, IN, USA), cooled to -80°C , and cut into 5 μ m sections using a cryostat (Leica, Heidelberg, Germany). Frozen sections were fixed for 10 minutes in cold acetone. Intrarenal expression levels of fibroblast-specific protein 1 (FSP-1; Abcam, Cambridge, UK), α -smooth muscle actin (α SMA, Abcam), and CD31 (Abcam) were measured by confocal microscopy.

Alexa Fluor[®] 488-conjugated goat anti-rabbit antibody (Molecular Probes, Eugene, OR, USA), Alexa Fluor[®] 555-conjugated anti-rat antibody, and Alexa Fluor[®] 555-conjugated anti-mouse antibody were used as secondary antibodies. All sections were washed and incubated for an additional 5 minutes with 4',6-diamidino-2-phenylindole for counterstaining. For negative controls, primary antibodies were omitted from the staining procedure.

Immunofluorescence analysis of FSP-1 and von Willebrand factor (vWF; Abcam) was carried out using cytospin preparations, generated by centrifugation of 200 μ L of cell suspension for 3 minutes at 1,000 rpm onto conventional glass slides using a Shandon Cytospin III cytocentrifuge (Thermo Shandon Ltd., Cambridge, UK).

Immunofluorescence analysis of HUVECs and hTECs

in culture was carried out as follows. Cultured HUVECs and hTECs in 8-well-chamber slides were fixed with 2% paraformaldehyde for 5 minutes and then washed twice with PBS. HUVECs were stained for CD31 and FSP-1, and hTECs were stained for E-cadherin (Abcam) and FSP-1. The slides were then fixed with 2% paraformaldehyde for 5 minutes and washed twice with PBS.

Quantitation of epoxyoctadecenoic acid (EpOME) and dihydroxyoctadec-12-enoic acid (DHOME)

In vivo sEH activity was evaluated by measuring the concentrations of EpOME and DHOME using a validated high-performance liquid chromatography/mass spectrometry/mass spectrometry method as described previously [7,8]. Briefly, a 200 μ L plasma sample was spiked with 50 μ L of internal standard (200 ng/mL of $[\pm]$ 12,13 DHOME d4), and 2 mL of diethyl ether was added to each sample for liquid–liquid extraction. Detection was performed using an API-4000 QTRAP (Applied Biosystems, Foster City, CA, USA). Eleven working standards were used: 500, 250, 150, 100, 50, 25, 10, 5, 1, 0.5, and 0.1 ng/mL.

Measurement of EETs

Culture supernatants were collected, and the antioxidant reagent triphenylphosphine was added. Aliquots were kept at -80°C until analysis. EET concentration was measured using a 14,15-EETs/DHET ELISA kit (Detroit R&D, Detroit, MI, USA).

Quantitative real-time polymerase chain reaction

Total RNA was extracted from kidney tissues harvested from mice 1 or 2 weeks after induction of UUO. Cytokine mRNA concentrations were assayed by polymerase chain reaction (PCR). Briefly, total RNA was isolated from kidneys using an RNeasy[®] kit (Qiagen GmbH, Hilden, Germany), and 1 μ g of total RNA was reverse-transcribed using oligo-d(T) primers and AMV-RT Taq polymerase (Promega, Madison, WI, USA). Real-time PCR was performed using Assay-on-Demand TaqMan[®] probes and primers for FSP-1, TGF- β 1, TGF- β 2, vWF, CD31, VE-cadherin, c-kit, and glyceraldehyde 3-phosphate dehydrogenase (*GAPDH*) (Applied Biosystems) on an ABI PRISM[®]

7500 Sequence Detection System (Applied Biosystems). The levels of mRNA expression for each cytokine were normalized to the level of *GAPDH* mRNA in the same sample.

Western-blot analysis

EndMT and EMT protein levels were analyzed by immunoblotting. Primary antibodies against FSP-1, α SMA, Collagen-4 (Abcam), CD31 (Santa Cruz Biotechnologies, Santa Cruz CA, USA), E-cadherin (Abcam), and β -actin (Sigma-Aldrich, St. Louis, MO, USA) were used for immunoblotting. Briefly, equal amounts (80 μ g) of extracted proteins were separated by 10% sodium dodecyl sulfate–polyacrylamide gel electrophoresis and transferred onto Immobilon-FL 0.4 μ M polyvinylidenedifluoride membranes (Millipore, Bedford, MA, USA). Anti-rabbit IgG (Vector Laboratories, Burlingame, CA, USA) was used as the secondary antibody. Blots were developed using Super Signal West Pico Chemiluminescent Substrate (Pierce, Woburn, MA, USA).

Flow-cytometry analysis

For quantitative flow-cytometry analysis, intrarenal mononuclear cells were isolated from mouse kidney homogenates using a Stomacher[®] 80 Biomaster (Seward Ltd., Worthing, Sussex, UK). Single-cell suspensions were created by passing tissues through a 40 μ m cell strainer. Kidneys were resuspended in 36% Percoll (Amersham Pharmacia Biotech, Piscataway, NJ, USA) and overlaid onto 72% Percoll. After centrifugation for 30 minutes at 1,000 g at 25°C, kidney mononuclear cells were isolated from the interface. Isolated kidney mononuclear cells were incubated with fluorophore-conjugated mouse monoclonal antibodies against CD31 and FSP-1 (Bioss, Woburn, MA, USA). Quantitative fluorescence analysis was performed using a FACSCalibur instrument and CellQuest software (BD Biosciences, Franklin Lakes, NJ, USA).

Statistical analysis

All data are expressed as mean \pm standard error of mean (SEM). Group means were compared using the Mann-Whitney *U* test, one-way ANOVA followed by Tukey's *post-hoc* analysis, or two-way ANOVA followed by Bonferroni *post-hoc* analysis as appropriate. All statistical analyses were performed using GraphPad Prism[®]

version 4 (GraphPad Software, Inc., La Jolla, CA, USA). *P* value less than 0.05 was considered to represent statistically significant differences.

Results

Inhibition of sEH activity reduces kidney fibrosis

We first quantitated the degree of kidney fibrosis induced by UUO in mice using Masson's trichrome staining. There was extensive tubulointerstitial fibrosis two weeks after UUO; however, AUDA-treated UUO mice exhibited reduced interstitial fibrosis (Fig. 1A, B). To further test the notion that administration of AUDA reduced kidney fibrosis, we performed immunofluorescence analyses. In UUO mice, we detected FSP-1 and α SMA, a marker of fibrosis, in both interstitial and tubule cells. In some instances, we found co localization of FSP-1 and α SMA with CD31, an endothelial cell marker (Fig. 1C–H). Such co-expression of fibroblastic and endothelial markers was interpreted as an indication that cells were undergoing EndMT. In addition to fibroblast proliferation, we also observed destruction of the peritubular capillary network of the kidney in UUO mice. AUDA treatment significantly reduced the level of FSP-1–positive tubulointerstitial fibrosis. Specifically, the numbers of FSP-1/CD31 double-positive fibroblasts and α SMA/CD31 double-positive fibroblasts were considerably decreased after treatment of UUO mice with AUDA. Furthermore, AUDA treatment preserved the peritubular capillary network. With respect to the mRNA level (as determined by real-time PCR) and protein level (as determined by immunoblotting), we quantitatively confirmed that inhibition of sEH down-regulated the expression of FSP-1 (Fig. 1I, J). Blood pressure, monitored non-invasively, was not significantly affected by AUDA treatment (Supplementary fig. 1).

Plasma EpOME and EpOME/DHOME ratio are elevated by sEH inhibition in UUO

sEH catalyzes the conversion of EpOME to DHOME. To investigate the *in vivo* activity of sEH, we measured the plasma concentrations of EpOME and DHOME (*n* = 6 per group). UUO had no effect on the plasma concentration of either compound. However, 9,10-, and total EpOME concentrations were significantly elevated in response to

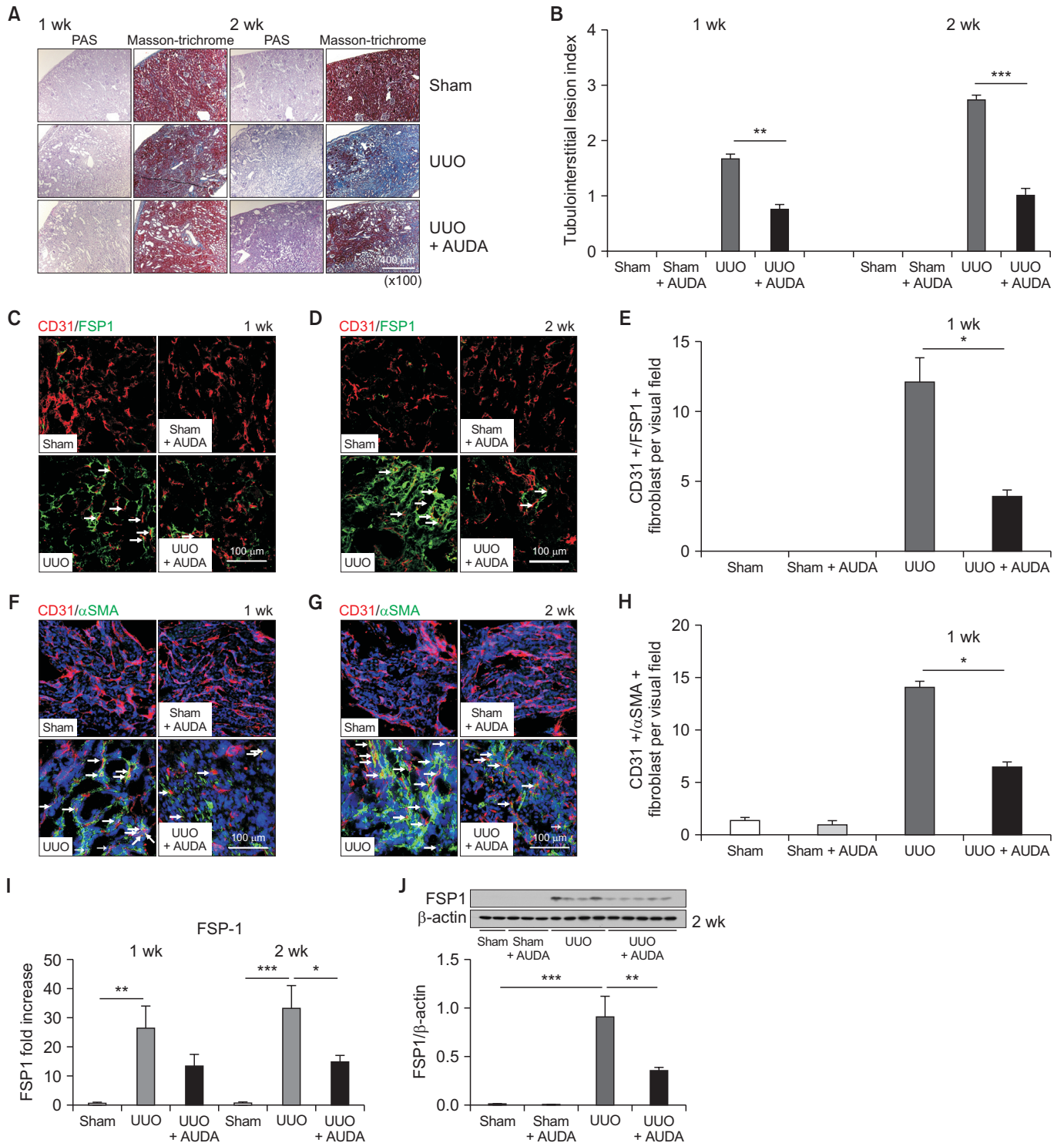


Figure 1. Effects of soluble epoxide hydrolase (sEH) inhibition on kidney tubulointerstitial fibrosis. (A, B) Significantly reduced interstitial fibrosis following treatment with 12-(3-adamantan-1-ylureido)-dodecanoic acid (AUDA) in a unilateral ureteral obstruction (UUO) model. (C–E) Immunofluorescence analysis. AUDA significantly reduced the level of fibroblast-specific protein 1 (FSP-1) positive fibrosis, the proportion of FSP-1/CD31-positive cells, and preserved the peritubular capillary network. Arrows indicate FSP-1/CD3 double-positive cells. (F–H) AUDA also reduced the level of αSMA-positive fibrosis and the proportion of αSMA/CD31 double-positive cells. (I, J) Inhibition of sEH down-regulated expression of FSP-1 as demonstrated by real-time PCR (I) and Western blotting (J). Values are given as mean ± standard error of mean (n = 6 per group for each experiment).

P* < 0.05, *P* < 0.01, ****P* < 0.001; by ANOVA test.

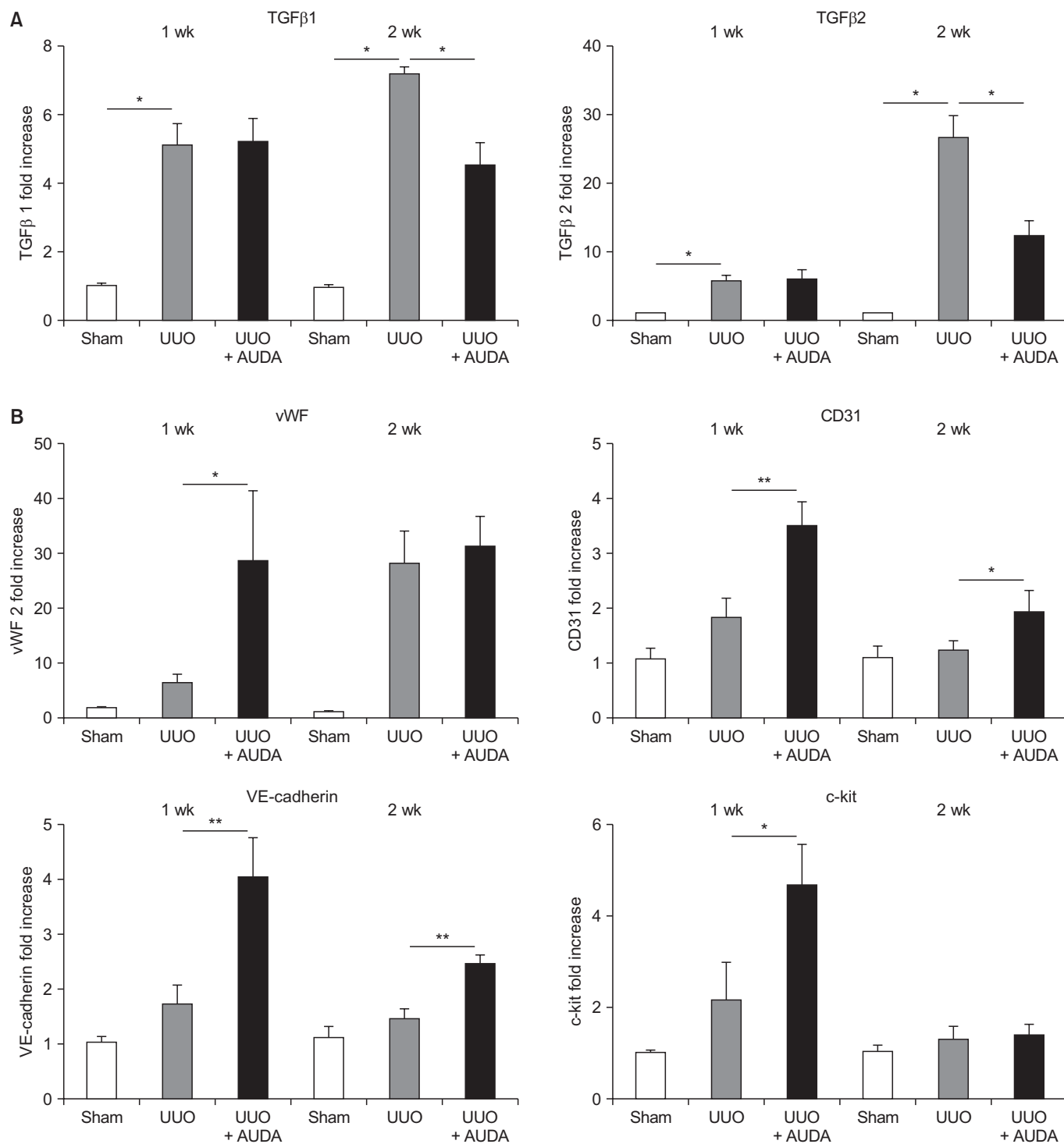


Figure 2. Alteration of the microenvironment by soluble epoxide hydrolase inhibition in a unilateral ureteral obstruction (UUO) model. 12-(3-adamantan-1-ylureido)-dodecanoic acid (AUDA) treatment suppressed transforming growth factor (TGF)-β1 and TGF-β2 (A) and increased expression of angiogenic molecules such as von Willebrand factor (vWF), CD31, and VE-cadherin (B). Values are given as mean ± standard error of mean (n = 6 per group for each experiment). *P < 0.05, **P < 0.01; by ANOVA test.

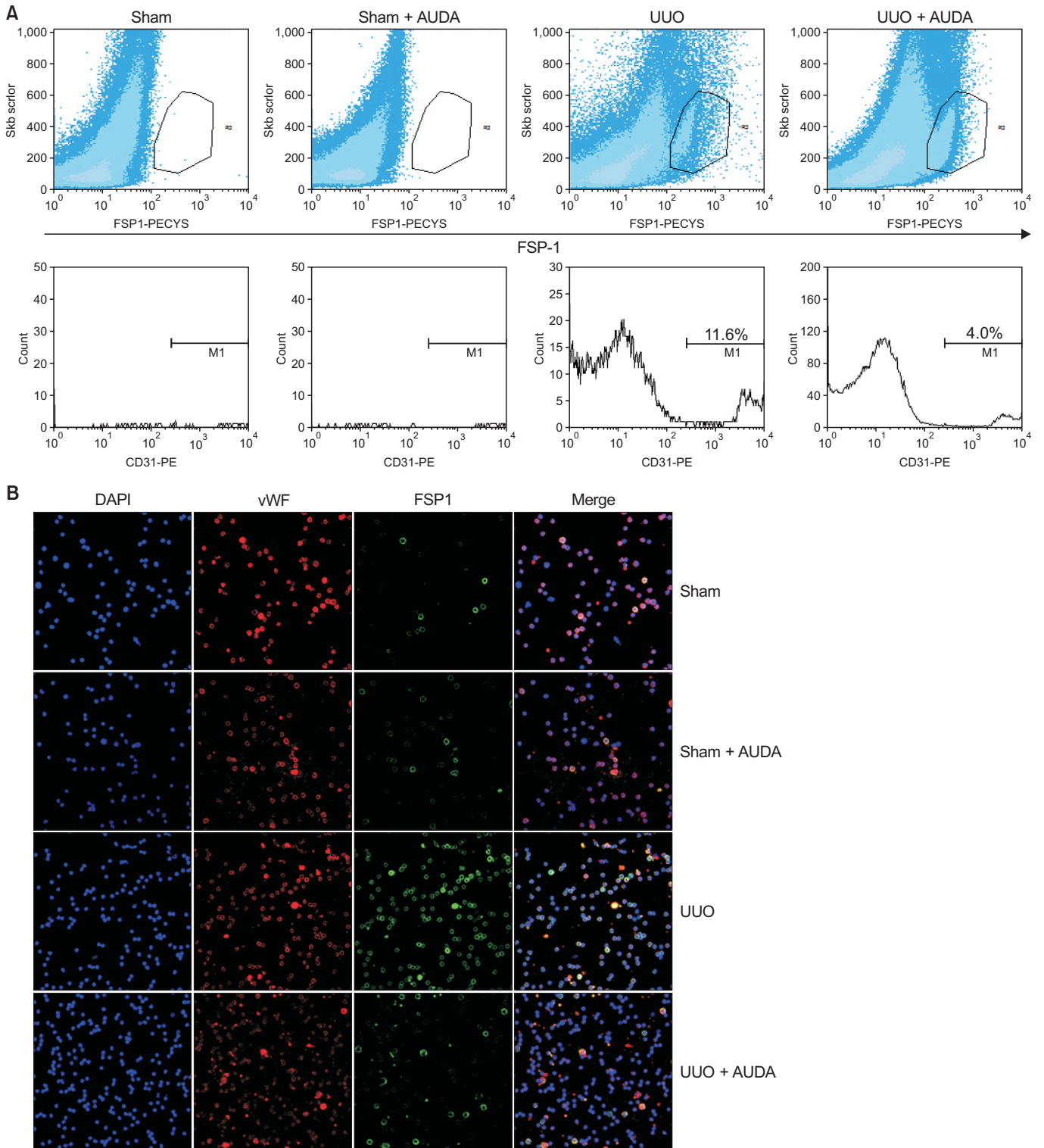


Figure 3. Regulation of endothelial-to-mesenchymal transition by soluble epoxide hydrolase inhibition in a unilateral ureteral obstruction (UUO) model. (A) Flow-cytometric analysis. The proportion of fibroblast-specific protein 1 (FSP-1)/CD31 double-positive cells among all FSP-1–positive cells was reduced by 12-(3-adamantan-1-ylureido)-dodecanoic acid (AUDA) treatment. (B) Immunofluorescence analyses of CD31 cells from isolated intrarenal mononuclear cells obtained from cytospin preparations. AUDA treatment reduced the proportion of von Willebrand factor/FSP-1 double-positive cells.

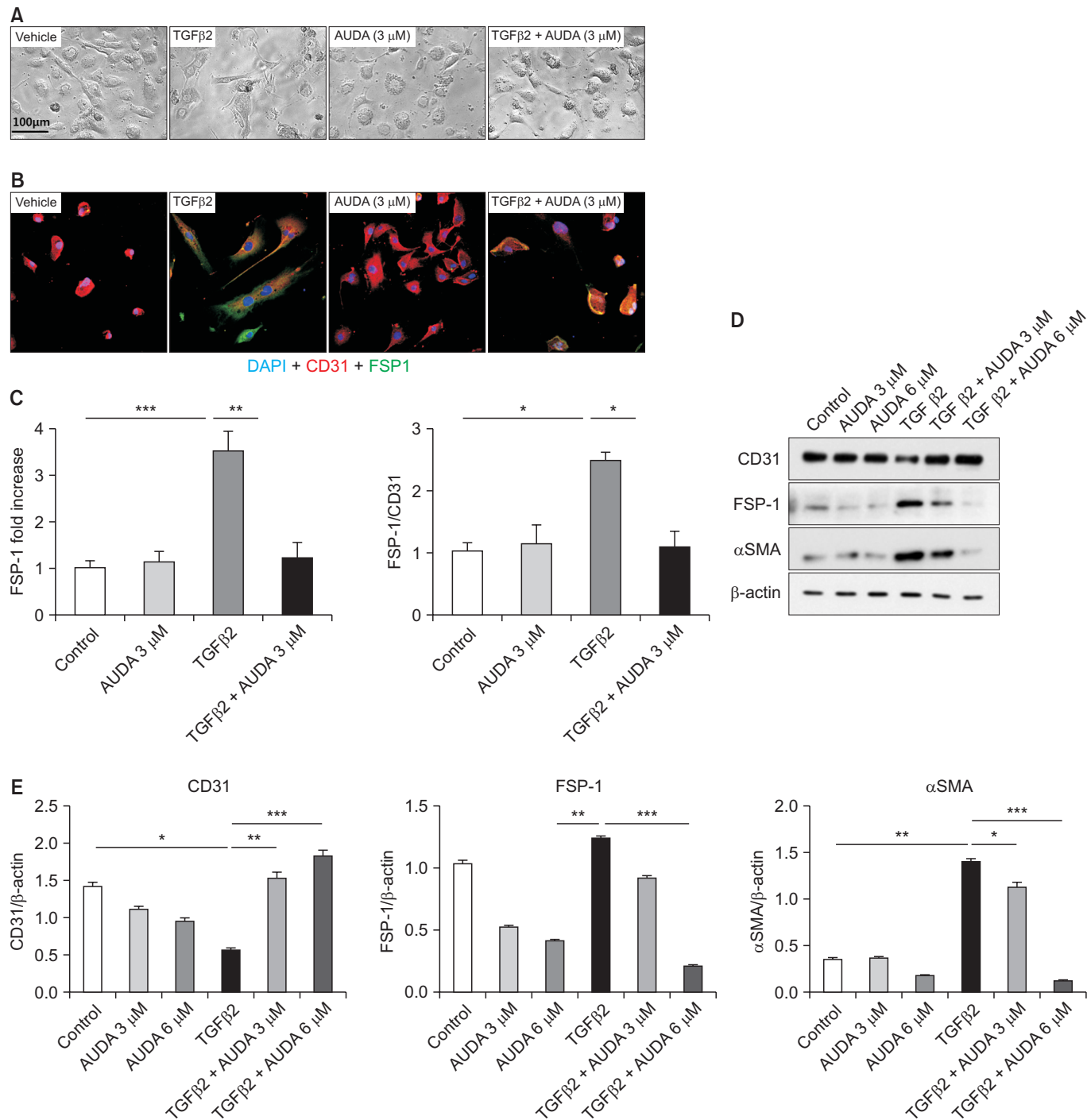


Figure 4. Regulation of endothelial-to-mesenchymal transition by soluble epoxide hydrolase inhibition in an *in vitro* model using human umbilical vein endothelial cells (HUVECs). (A, B) Recombinant transforming growth factor (rTGF)-β2–induced fibroblast-like changes and fibroblast-specific protein 1 (FSP-1) expression in HUVECs were reversed by 12-(3-adamantan-1-ylureido)-dodecanoic acid (AUDA) treatment. (C–E) AUDA treatment increased expression of CD31 and reduced expression of αSMA and FSP-1. All values are given as mean ± standard error of mean (n = 4 per group for each experiment). **P* < 0.05, ***P* < 0.01, ****P* < 0.001; by ANOVA test.

sEH inhibition by AUDA following UO (Supplementary fig. 2). No significant changes were observed for DHOME plasma concentrations following treatment with AUDA.

sEH inhibition changes the microenvironment in injured kidneys

To investigate the mechanism underlying the milder interstitial kidney fibrosis observed in AUDA-treated UO mice, we quantitated TGF-β expression by real-time PCR (Fig. 2A). This analysis revealed that TGF-β1 and TGF-β2 were upregulated at the mRNA level following UO in C57BL/6 mice; however, TGF-β expression was significantly suppressed after 2 weeks of AUDA treatment.

In addition, we assessed the expression patterns of

molecules associated with activation of endothelial cells, including vWF, CD31, and VE-cadherin (Fig. 2B). The expression of these molecules was upregulated by UO, although the differences were not significant and were increased further by AUDA administration. c-kit (CD117), a cytokine receptor expressed on the surface of hematopoietic stem cells, was also significantly upregulated by AUDA.

sEH contributes to kidney fibrosis by promoting EndMT and EMT

We further confirmed that sEH inhibition reduces EndMT by flow-cytometric and immunofluorescence analyses of cytospin preparations. Flow-cytometric analysis

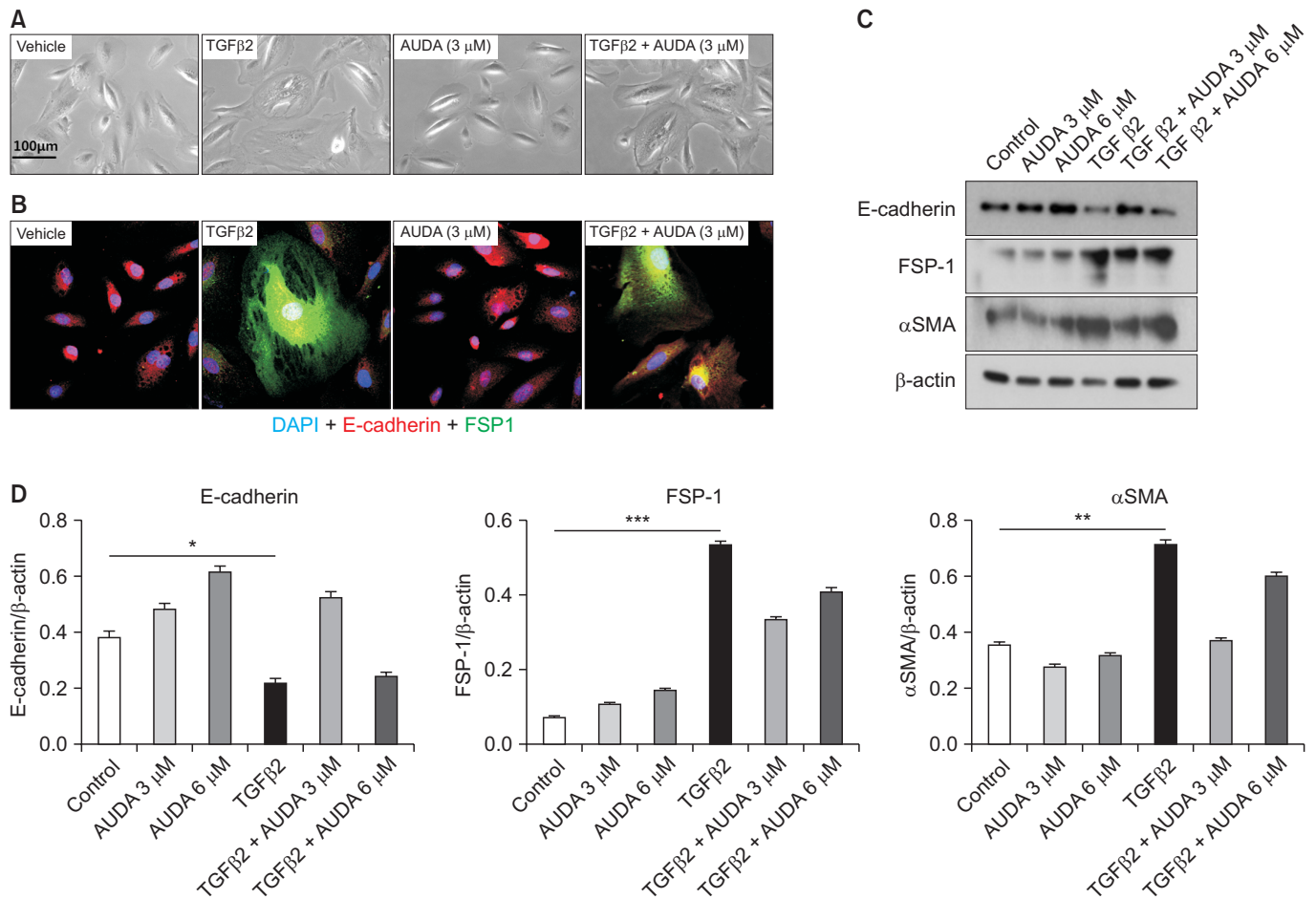


Figure 5. Direct effect of soluble epoxide hydrolase inhibition on epithelial-to-mesenchymal transition (EMT) in an *in vitro* model using human kidney tubular epithelial cells (TECs). (A–D) Recombinant transforming growth factor (rTGF)-β2–induced EMT of TECs was not reversed by 12-(3-adamantan-1-ylureido)-dodecanoic acid (AUDA) treatment.

FSP-1, fibroblast-specific protein 1.

P* < 0.05, *P* < 0.01, ****P* < 0.001; by ANOVA test.

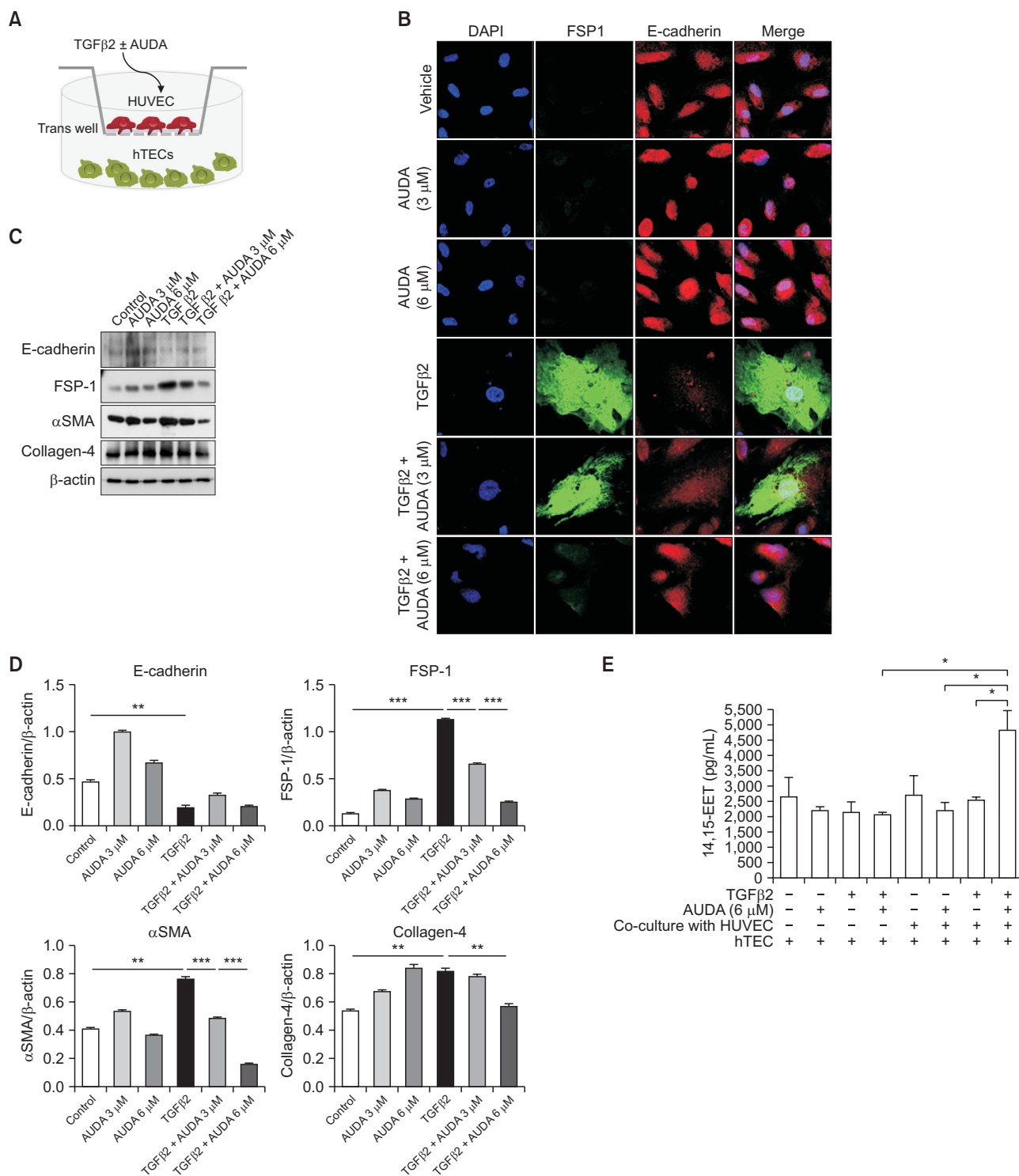


Figure 6. Indirect effect of soluble epoxide hydrolase inhibition on epithelial-to-mesenchymal transition (EMT) in an *in vitro* co-culture model of human kidney tubular epithelial cells (hTECs) and human umbilical vein endothelial cells (HUVECs). (A) Co-culture of TECs and HUVECs using the Transwell™ system. (B–D) Activation of HUVECs by 12-(3-adamantan-1-ylureido)-dodecanoic acid treatment reversed recombinant transforming growth factor (rTGF)-β2-induced fibroblast-like changes and expression of FSP-1, αSMA, and collagen-4 in TECs. (E) The concentration of 14,15-EET-epoxyeicosatrienoic acids (EETs) in culture supernatants. Values are given as mean ± standard error of mean (n = 4 per group for each experiment). AUDA, 12-(3-adamantan-1-ylureido)-dodecanoic acid. *P < 0.05, **P < 0.01, ***P < 0.001; by ANOVA test.

demonstrated that the proportion of FSP-1–positive cells was increased in the UUO group relative to the sham-operated group (Fig. 3A). In addition, treatment of UUO mice with AUDA reduced the proportion of CD31/FSP1 double-positive cells in the FSP-1–positive population. We next sorted CD31 cells from isolated intrarenal mononuclear cells obtained from mouse kidney homogenates, generated cytospin preparations, and performed double staining for vWF (red) and FSP-1 (green) (Fig. 3B). Cells positive for both vWF and FSP-1 were more abundant in UUO mice, but inhibition of sEH by AUDA reduced the proportion of vWF/FSP-1 double-positive cells.

Histological examination confirmed that fibrosis was ameliorated by AUDA treatment (Fig. 1A). Specifically, AUDA increased the expression of endothelial markers such as vWF, VE-cadherin, and CD31, but decreased expression of TGF- β and FSP-1 (Fig. 2). However, EndMT, as reflected by co-localization of CD31/FSP-1 and CD31/ α SMA, is only one aspect of interstitial fibrosis (Fig. 1C–H).

To evaluate the mechanisms by which AUDA reduces tubulointerstitial fibrosis in addition to EndMT, we next performed *in vitro* studies. Using an *in vitro* EndMT model, we found that rTGF- β 2 treatment caused HUVECs to assume a fibroblast-like morphology and express a high level of FSP-1 (Fig. 4). AUDA treatment prevented this morphological change and reduced expression of FSP-1. Furthermore, AUDA significantly increased the expression of CD31, while reducing expression of smooth muscle actin and FSP-1.

We repeated similar studies in hTEC to evaluate the direct effects of AUDA on EMT (Fig. 5). rTGF- β 2 induced morphological changes in TECs, decreased expression of the epithelial cell marker E-cadherin, and increased the level of FSP-1. However, inhibition of sEH did not prevent EMT in cultures that did not contain endothelial cells. To test the possibility that AUDA treatment could reduce EMT of TECs co-cultured with endothelial cells, we grew TECs and HUVECs in separate chambers using the Transwell™ system (Thermo Fisher Scientific, Roskilde, Denmark) (Fig. 6A). Similar to single cultures of TECs, rTGF- β 2 induced EMT in co-cultivated TECs, while AUDA-activated HUVECs prevented EMT in a dose-dependent manner (Fig. 6B–D).

We next measured the concentrations of EETs in culture supernatants (Fig. 6E). AUDA treatment significantly increased the concentration of EET in co-cultures of

TECs and HUVECs, but did not affect EET concentration in single cultures of TECs in the absence of endothelial cells. Taken together, these findings suggest that the sEH inhibitor AUDA reduces EMT of TECs by increasing the concentration of EET in vascular endothelial cells.

Discussion

Kidney fibrosis is regarded as the final common pathway of end stage kidney disease. Therefore, identifying the mechanism by which fibrosis develops in end-stage kidney disease and developing ways to prevent or reverse this process is desirable. Although there have been many studies directed toward these goals, no effective treatment for fibrosis has been developed. In the present study, we investigated the role of specific inhibition of sEH in tubulointerstitial kidney fibrosis caused by UUO. Importantly, inhibition of sEH can reduce kidney fibrosis by preventing EndMT and EMT, thereby preserving the peritubular capillary network.

Infiltration of inflammatory cells such as macrophages, apoptosis or necrosis of tubular cells, and proliferation of resident interstitial fibroblasts all actively contribute to the process of renal tissue deterioration [15]. Over the past few years, EMT has been recognized as an important mechanism of fibrosis [16,17]. Infiltrating macrophages produce cytokines such as TGF- β 1 that promote EMT. Moreover, endothelial cells themselves can differentiate into mesenchymal cells under stress conditions and are therefore a major source of fibroblasts [3]. The cytokine TGF- β 2 plays an important role in directing the transformation of endothelial to fibroblast-like cellular phenotypes [18]. Zeisberg et al [19] demonstrated that bone morphogenetic protein-7 inhibits EndMT in cardiac fibrosis, both *in vitro* and *in vivo*, and suggested that EndMT represents a new therapeutic target for fibrosis. However, only a few studies have focused on EndMT as an important mechanism in chronic kidney disease [20,21]. To the best of our knowledge, this is the first study in which kidney fibrosis has been successfully alleviated through regulation of EndMT.

Kidney EETs, which act as EDHFs, are involved in regulation of kidney blood flow and long-term control of arterial blood pressure [6,22]. Furthermore, sEH plays a central role in the regulation of EET concentrations, and sEH inhibitors have been shown to be effective for the treatment or prevention of acute cardiovascular and

kidney diseases. However, the effects of sEH inhibitors in chronic disease have not been thoroughly elucidated. A recent study of postmyocardial infarction demonstrated that sEH inhibition can reduce cardiac fibrosis and has a beneficial effect on remodeling [23]; however, the effect of sEH in chronic kidney disease remains controversial [24]. Here, we showed that inhibition of sEH prevented tubulointerstitial kidney fibrosis in a UUO model by several potential mechanisms.

First, we showed that inhibition of sEH prevented TGF- β 2-induced EndMT of endothelial cells. Zeisberg et al [21] reported that 36% of all FSP-1-positive cells and 25% of all α SMA-positive cells in a UUO model co-express the endothelial marker CD31; however, in our study, only 11.6% of FSP-1-positive cells and 14.0% of α SMA-positive cells co-expressed CD31. A recent study demonstrated that pericytes are another important source of fibroblasts [25]; thus, the discrepancy in results could be due to the exclusive use of confocal microscopy by Zeisberg et al [21] in their analyses, possibly resulting in overestimation. In addition, we found that inhibition of sEH prevented kidney fibrosis via mechanisms other than direct control of the EndMT. Specifically, sEH inhibition resulted in upregulation of angiogenic molecules such as c-kit and vWF, with improved preservation of intrarenal peritubular microvascular structures. We previously reported that inhibition of sEH increases the expression of molecules associated with endothelial cell migration and neovascularization such as c-kit (CD117) in a model of ischemia-reperfusion injury [8]. Interstitial fibrosis increases as the number of peritubular capillaries decreases [26], and loss of peritubular capillaries precedes interstitial fibrosis and glomerulosclerosis [27]. In this way, destabilization of peritubular capillaries can lead to capillary loss and fibrosis [25].

Lastly, we demonstrated that sEH inhibition could attenuate EMT indirectly. A previous study reported that EET treatment of TECs reverses TGF- β 1-induced EMT by modulating TGF- β 1/Smad signaling [28]. Here, we showed that sEH inhibition had no effect on reducing EMT of TECs cultured alone; however, when TECs were co-cultured with endothelial cells, AUDA significantly reduced the extent of EMT in these cells. Thus, EETs produced by endothelial cells might prevent fibrotic changes of TECs. Taken together, our data demonstrate that endothelial dysfunction in the kidney contributes to

the development of tubulointerstitial fibrosis by several mechanisms. Therefore, regulation of sEH activity represents a potential target for therapies aimed at delaying the progression of fibrosis associated with chronic kidney disease.

Conflicts of interest

All authors have no conflicts of interest to declare.

Acknowledgments

This work was supported by a grant from the Korea Healthcare Technology R&D Project, Ministry for Health and Welfare, Republic of Korea (HI11C1291), and by a grant from the Korean Society of Nephrology (BAXTER, 2011).

Supplementary materials

Further details are presented in the online version of this article (available at <https://doi.org/10.23876/j.krcp.2017.36.4.329>).

References

- [1] Eddy AA. Molecular basis of renal fibrosis. *Pediatr Nephrol* 15:290-301, 2000
- [2] Iwano M, Plieth D, Danoff TM, Xue C, Okada H, Neilson EG. Evidence that fibroblasts derive from epithelium during tissue fibrosis. *J Clin Invest* 110:341-350, 2002
- [3] Medici D, Shore EM, Lounev VY, Kaplan FS, Kalluri R, Olsen BR. Conversion of vascular endothelial cells into multipotent stem-like cells. *Nat Med* 16:1400-1406, 2010
- [4] Zeisberg EM, Tarnavski O, Zeisberg M, et al. Endothelial-to-mesenchymal transition contributes to cardiac fibrosis. *Nat Med* 13:952-961, 2007
- [5] Campbell WB, Gebremedhin D, Pratt PF, Harder DR. Identification of epoxyeicosatrienoic acids as endothelium-derived hyperpolarizing factors. *Circ Res* 78:415-423, 1996
- [6] Imig JD. Epoxide hydrolase and epoxygenase metabolites as therapeutic targets for renal diseases. *Am J Physiol Renal Physiol* 289:F496-F503, 2005
- [7] Lee JP, Yang SH, Kim DK, Lee H, Kim B, Cho JY, et al. In vivo activity of epoxide hydrolase according to sequence variation affects the progression of human IgA nephropathy. *Am*

- J Physiol Renal Physiol* 300:F1283-F1290, 2011
- [8] Lee JP, Yang SH, Lee HY, et al. Soluble epoxide hydrolase activity determines the severity of ischemia-reperfusion injury in kidney. *PLoS One* 7:e37075, 2012
- [9] McPherson C. Regulation of animal care and research? NIH's opinion. *J Anim Sci* 51:492-496, 1980
- [10] Kim IH, Nishi K, Tsai HJ, et al. Design of bioavailable derivatives of 12-(3-adamantan-1-yl-ureido)dodecanoic acid, a potent inhibitor of the soluble epoxide hydrolase. *Bioorg Med Chem* 15:312-323, 2007
- [11] Jung O, Brandes RP, Kim IH, et al. Soluble epoxide hydrolase is a main effector of angiotensin II-induced hypertension. *Hypertension* 45:759-765, 2005
- [12] Zhang W, Koerner IP, Noppens R, et al. Soluble epoxide hydrolase: a novel therapeutic target in stroke. *J Cereb Blood Flow Metab* 27:1931-1940, 2007
- [13] Gadola L, Noboa O, Márquez MN, et al. Calcium citrate ameliorates the progression of chronic renal injury. *Kidney Int* 65:1224-1230, 2004
- [14] Yang SH, Lee JP, Jang HR, et al. Sulfatide-reactive natural killer T cells abrogate ischemia-reperfusion injury. *J Am Soc Nephrol* 22:1305-1314, 2011
- [15] Wynn TA, Ramalingam TR. Mechanisms of fibrosis: therapeutic translation for fibrotic disease. *Nat Med* 18:1028-1040, 2012
- [16] Zeisberg M, Kalluri R. The role of epithelial-to-mesenchymal transition in renal fibrosis. *J Mol Med (Berl)* 82:175-181, 2004
- [17] Zeisberg M, Kalluri R. Fibroblasts emerge via epithelial-mesenchymal transition in chronic kidney fibrosis. *Front Biosci* 13:6991-6998, 2008
- [18] Sanford LP, Ormsby I, Gittenberger-de Groot AC, et al. TGFbeta2 knockout mice have multiple developmental defects that are non-overlapping with other TGFbeta knockout phenotypes. *Development* 124:2659-2670, 1997
- [19] Zeisberg EM, Potenta S, Xie L, Zeisberg M, Kalluri R. Discovery of endothelial to mesenchymal transition as a source for carcinoma-associated fibroblasts. *Cancer Res* 67:10123-10128, 2007
- [20] Li J, Qu X, Bertram JF. Endothelial-myofibroblast transition contributes to the early development of diabetic renal interstitial fibrosis in streptozotocin-induced diabetic mice. *Am J Pathol* 175:1380-1388, 2009
- [21] Zeisberg EM, Potenta SE, Sugimoto H, Zeisberg M, Kalluri R. Fibroblasts in kidney fibrosis emerge via endothelial-to-mesenchymal transition. *J Am Soc Nephrol* 19:2282-2287, 2008
- [22] Olearczyk JJ, Quigley JE, Mitchell BC, et al. Administration of a substituted adamantyl urea inhibitor of soluble epoxide hydrolase protects the kidney from damage in hypertensive Goto-Kakizaki rats. *Clin Sci (Lond)* 116:61-70, 2009
- [23] Kompa AR, Wang BH, Xu G, et al. Soluble epoxide hydrolase inhibition exerts beneficial anti-remodeling actions post-myocardial infarction. *Int J Cardiol* 167:210-219, 2013
- [24] Jung O, Jansen F, Mieth A, et al. Inhibition of the soluble epoxide hydrolase promotes albuminuria in mice with progressive renal disease. *PLoS One* 5:e11979, 2010
- [25] Kida Y, Duffield JS. Pivotal role of pericytes in kidney fibrosis. *Clin Exp Pharmacol Physiol* 38:467-473, 2011
- [26] Bohle A, Mackensen-Haen S, von Gise H, et al. The consequences of tubulo-interstitial changes for renal function in glomerulopathies. A morphometric and cytological analysis. *Pathol Res Pract* 186:135-144, 1990
- [27] Kang DH, Kanellis J, Hugo C, et al. Role of the microvascular endothelium in progressive renal disease. *J Am Soc Nephrol* 13:806-816, 2002
- [28] Chen G, Wang P, Zhao G, et al. Cytochrome P450 epoxygenase CYP2J2 attenuates nephropathy in streptozotocin-induced diabetic mice. *Prostaglandins Other Lipid Mediat* 96:63-71, 2011